



A distribution system state estimator accommodating large number of ampere measurements

Wenchuan Wu*, Yuntao Ju, Boming Zhang, Hongbin Sun

State Key Lab of Power Systems, Dept. of Electrical Engineering, Tsinghua University, Beijing, China

ARTICLE INFO

Article history:

Received 14 May 2011

Received in revised form 20 April 2012

Accepted 26 May 2012

Available online 15 July 2012

Keywords:

Robust state estimation

Distribution network

Branch current measurement

ABSTRACT

This paper presents a three-phase state estimation method for distribution network which can accommodate large number ampere measurements and voltage measurements. In this method, the power on sending end of branch and the square of branch current magnitude are chosen as the state variables. Therefore, measurement functions of ampere and voltage measurements are significantly simplified and no measurements transformation is needed in this method. Furthermore, a novel robust state estimation model is presented, which can suppress bad data automatically. The observability analysis indicates the proposed method can be used in distribution system with very limited measurements. Numerical tests on radial and weak-meshed network show the real-time branch current measurements can significantly improve the accuracy of estimation results.

© 2012 Elsevier Ltd. All rights reserved.

1. Introduction

Distribution system state estimation is used to estimate the system states with very limited real-time measurements. It is a critical module in modern distribution management system (DMS).

For a typical urban distribution system, there are many branch current measurements along the feeders with very few voltage and power measurements, which make distribution system state estimation problem very challenging. Many encouraging works have been done for distribution system. These methods can be roughly classified into three categories according to different state variables are used, which are suitable for different measurements configurations.

1.1. Node voltage based method [1,2]

In this type of methods, the node voltages are selected as state variables. And the power measurement and branch current magnitude measurements are transformed into equivalent branch and bus injection current vector to make the Jacobian matrix constant and improve calculation efficiency. Due to the measurement transformation, the weights of the real measurements and their corresponding transformed measurements are not equivalent, which may lead to extra errors in the estimation results.

1.2. Branch current vector based method [3,4]

Compared with the conventional node-voltage-based methods, the branch current vectors are selected as state variables in this type of methods. The voltage measurements are omitted and the power measurements and load pseudo-measurements are transformed into equivalent branch current vector and injection current vector by pre-calculated node voltage vectors. This method has good performance both in computation speed and memory requirements. The main shortage of the method is measurements transformation is needed, which may introduce extra errors. In Ref. [13], some special state variables are chosen to overcome this shortage, but this method can only be used for radial network.

1.3. Branch power based method [5,6]

In this type of methods, the whole problem is decomposed into a series of sub-problems and each sub-problem will deal with only single-branch state estimation. It is extremely efficient, but the solution of these methods cannot guarantee to global optimum.

Because of the limited number of real-time measurements in the distribution system, pseudo-measurements (especially the loads' pseudo-measurements) are necessary for distribution system state estimator. In Ref. [7], a Gaussian mixture model is used to formulate load probability distribution functions (PDFs), and the expectation maximization algorithm is used to obtain the parameters of the mixture components. The loads' pseudo-measurement is described as fuzzy number in [8]. Ref. [9] proposed a ARM based load estimation model according to the data recorded in automated meter

* Corresponding author.

E-mail address: wuwench@tsinghua.edu.cn (W. Wu).

reading (AMR) system. Ref. [10] presents a load modeling technique which incorporates the customers' billing information.

In this paper, a novel state estimation method is proposed, in which the branch current measurements and voltage measurements are directly formulated in a robust estimation model without measurements transformation. Due to the special chosen state variables, the measurement functions are quite simple. Furthermore, the proposed method can suppress bad data automatically when there are redundant ampere measurements. The proposed method is suitable both for radial and meshed distribution network with large number of branch current measurements.

The paper is organized as following. The estimation model and its measurement functions are introduced in Section 2. Section 3 presents an observability analysis for this proposed method. Numerical tests both for radial and weakly meshed distribution networks are given in Section 4, followed by a conclusion in Section 5.

2. Problem modeling

The following symbols are used in this paper:

- \mathbf{I}_{ij} is three phase branch $i-j$ current magnitude vector;
- $\mathbf{A}_{ij} [I_{ij(a)}^2 \ I_{ij(b)}^2 \ I_{ij(c)}^2]^T$ is three phase square of branch $i-j$ current magnitude vector; $I_{ij(a)}^2, I_{ij(b)}^2, I_{ij(c)}^2$ are square of phase a, b or c current magnitude respectively.
- $\mathbf{P}_{ji}, \mathbf{Q}_{ji}$ are three phase active and reactive power vector on the sending end of branch $i-j$ (i represents the sending node);
- $\mathbf{P}_{ji}, \mathbf{Q}_{ji}$ are three phase active and reactive power vector on the receiving end of branch $i-j$ (j represents the receiving node).
- \mathbf{V}_i is three phase voltage magnitude vector of node i .
- $\mathbf{P}_{ji}, \mathbf{Q}_{ji}$ are three phase injection active and reactive power vector of node i .
- \mathbf{Z}_{ij} are the impedance matrix of branch $i-j$ with phases.
- \mathbf{X}_{ci} is the shunt reactance matrix at node i including line charging and any shunt capacitive or inductive reactance; $(\cdot)^m$ denotes measurement.

The power on sending end of branch $\mathbf{P}_{ij}, \mathbf{Q}_{ij}$ and the square of branch current magnitude \mathbf{A}_{ij} are chosen as the state variables in this method. To make more readable, a superscript x is used to mark the state variables. For example, $\mathbf{P}_{ij}^x, \mathbf{Q}_{ij}^x$ and \mathbf{A}_{ij}^x represent the power on sending end of branch and the square of branch current magnitude respectively.

2.1. Robust estimation model

Distribution system state estimation is to solve an over-determined set of nonlinear equations as:

$$\mathbf{z} = \mathbf{h}(\mathbf{x}) + \mathbf{e} \quad (1)$$

where \mathbf{x} is the state vector, the element is $\mathbf{P}_{ij}^x, \mathbf{Q}_{ij}^x$ or \mathbf{A}_{ij}^x in this paper; \mathbf{z}, \mathbf{h} and \mathbf{e} are $m \times 1$ measurement vector, measurement function vector and measurement error vector respectively.

A robust state estimation model with ability to suppress bad data, which is formulated as an optimization problem with an exponential square objective function:

$$\begin{aligned} \max_{\mathbf{x}} J(\mathbf{x}) &= \sum_{i=1}^m w_i \exp\left(-\frac{(z_i - h_i(\mathbf{x}))^2}{2\sigma^2}\right) \\ &= \sum_{i=1}^m w_i \exp(-r_{si}^2) \\ \text{s.t. } \quad \mathbf{c}(\mathbf{x}) &= \mathbf{0} \end{aligned} \quad (2)$$

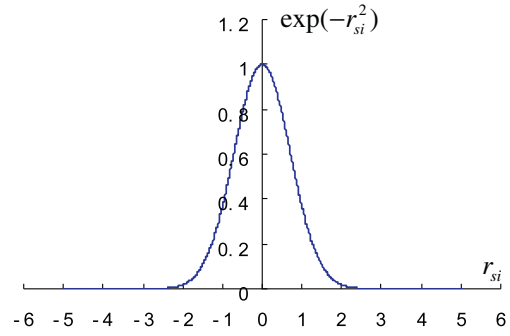


Fig. 1. Exponential square objective function for $\exp(-r_{si}^2)$.

where w_i is the weight for i th measurement, σ is a constant number, $r_{si} = (z_i - h_i(\mathbf{x}))/\sqrt{2}\sigma$ is the weighted residual error. $\mathbf{c}(\mathbf{x}) = \mathbf{0}$ is the $\mathbf{p} \times 1$ zero injection vector equation and other equality constraints.

It can be seen from (2) that this estimator is a special M -estimator. The objective function in (2) is continuously differentiable, so conventional optimization methods can be used. On the other hand, this function has an interesting property which leads to a strong ability to suppress bad data.

$\exp(-r_{si}^2)$ in (2) can be depicted with line as shown in Fig. 1. For a bad measurement, its residual $|r_{si}|$ will be relatively large, so $\exp(-r_{si}^2) \approx 0$. So measurements with large residual error will not affect estimation results, which ensure the robustness of the method.

2.2. Estimation model for radial network

For a radial distribution system as shown in Fig. 2, the state variables are $\mathbf{P}_{ij}^x, \mathbf{Q}_{ij}^x$ and \mathbf{A}_{ij}^x ($i = 1, 2, \dots, n-1; j = 2, 3, \dots, n$).

The measurement functions used in the proposed estimation model (2) can be described as followings:

- (1) Branch current measurement function

$$(\mathbf{A}_{ij})^m = \mathbf{A}_{ij}^x \quad (3)$$

- (2) Function of power measurement on sending end of branch

$$(\mathbf{P}_{ij})^m = \mathbf{P}_{ij}^x \quad (4)$$

$$(\mathbf{Q}_{ij})^m = \mathbf{Q}_{ij}^x \quad (5)$$

- (3) Functions of power measurement on receiving end of branch

$$(\mathbf{P}_{ji} + j\mathbf{Q}_{ji})^m = \mathbf{P}_{ij}^x + j\mathbf{Q}_{ij}^x - \mathbf{A}_{ij}^x \mathbf{Z}_{ij} \quad (6)$$

- (4) Node injection power measurement functions

$$\begin{aligned} (\mathbf{P}_j + j\mathbf{Q}_j)^m &= \sum_{i \in j} (\mathbf{P}_{ij}^x + j\mathbf{Q}_{ij}^x) - \sum_{i \in j} \mathbf{A}_{ij}^x \mathbf{Z}_{ij} - \sum_{k \in j} (\mathbf{P}_{jk}^x + j\mathbf{Q}_{jk}^x) \\ &\quad + j\mathbf{V}_j^2 \mathbf{X}_{cj} \end{aligned} \quad (7)$$

where, $i \in j$ represents node i is connected to node j ; $k \in j$ represents node k is connected to node j .

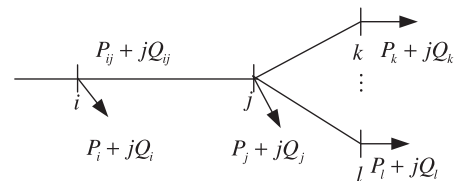


Fig. 2. Radial distribution network.

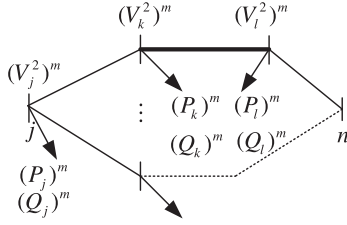


Fig. 3. Meshed distribution network.

(5) Square of voltage measurement function

$$(\mathbf{V}_j^2)^m = |\mathbf{P}_{jk}^x + j\mathbf{Q}_{jk}^x|^2 \text{diag} \left(\frac{1}{A_{jk(a)}^x}, \frac{1}{A_{jk(b)}^x}, \frac{1}{A_{jk(c)}^x} \right) \quad (8)$$

(6) Voltage constraint measurement function

$$0 = |\mathbf{P}_{ij}^x + j\mathbf{Q}_{ij}^x - \mathbf{A}_{ij}^x \mathbf{Z}_{ij}|^2 \text{diag} \left(\frac{1}{A_{ij(a)}^x}, \frac{1}{A_{ij(b)}^x}, \frac{1}{A_{ij(c)}^x} \right) - |\mathbf{P}_{jk}^x + j\mathbf{Q}_{jk}^x|^2 \text{diag} \left(\frac{1}{A_{jk(a)}^x}, \frac{1}{A_{jk(b)}^x}, \frac{1}{A_{jk(c)}^x} \right) \quad (9)$$

The voltage constraint measurement function (9), for each branch except the root branch, can be derived as following:

As shown in Fig. 3, there are two branches $i - j$ and $j - k$ connected to node j . The voltage of node j can both be calculated from branch $i - j$ and $j - k$ respectively:

$$\mathbf{V}_j^2 = |\mathbf{P}_{ij}^x + j\mathbf{Q}_{ij}^x - \mathbf{A}_{ij}^x \mathbf{Z}_{ij}|^2 \text{diag} \left(\frac{1}{A_{ij(a)}^x}, \frac{1}{A_{ij(b)}^x}, \frac{1}{A_{ij(c)}^x} \right) \quad (10)$$

$$\mathbf{V}_j^2 = |\mathbf{P}_{jk}^x + j\mathbf{Q}_{jk}^x|^2 \text{diag} \left(\frac{1}{A_{jk(a)}^x}, \frac{1}{A_{jk(b)}^x}, \frac{1}{A_{jk(c)}^x} \right) \quad (11)$$

Combined Eqs. (10) and (11), Eq. (9) can be derived. This equation should be both formulated as measurement function $\mathbf{h}(\mathbf{x})$ and equality constraint $\mathbf{c}(\mathbf{x})$ in the state estimation model (2).

In this estimation model, there are nine unknown variables ($\mathbf{A}_{ij}^x, \mathbf{P}_{ij}^x, \mathbf{Q}_{ij}^x$) for each branch, so three extra unknown variables existed than conventional method. Fortunately, there is three extra voltage constraint measurement functions (defined in Eq. (9)) for each branch with three phases, so these extra unknown variables do not affect the system's observability.

2.3. Estimation model for meshed network

A meshed network as shown in Fig. 3 can be translated into equivalent radial network as shown in Fig. 4 by adding breakpoints to open loops [11].

For a meshed network, following measurement functions should be added for the estimation model according to the equivalent network as shown in Fig. 4.

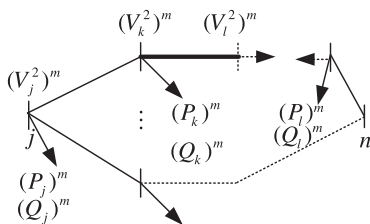


Fig. 4. Equivalent radial distribution network with breakpoints.

(1) Voltage measurement function of break point

$$(\mathbf{V}_l^2)^m = |\mathbf{P}_{kl}^x + j\mathbf{Q}_{kl}^x|^2 \text{diag} \left(\frac{1}{A_{kl(a)}^x}, \frac{1}{A_{kl(b)}^x}, \frac{1}{A_{kl(c)}^x} \right) \quad (12)$$

(2) Voltage constraint measurement function of break point

$$|\mathbf{P}_{kl}^x + j\mathbf{Q}_{kl}^x - \mathbf{A}_{kl}^x \mathbf{Z}_{kl}|^2 \text{diag} \left(\frac{1}{A_{kl(a)}^x}, \frac{1}{A_{kl(b)}^x}, \frac{1}{A_{kl(c)}^x} \right) = |\mathbf{P}_{nl}^x + j\mathbf{Q}_{nl}^x - \mathbf{A}_{nl}^x \mathbf{Z}_{nl}|^2 \text{diag} \left(\frac{1}{A_{nl(a)}^x}, \frac{1}{A_{nl(b)}^x}, \frac{1}{A_{nl(c)}^x} \right) \quad (13)$$

This equation is formulated as equality constraint in the state estimation model.

(3) Injection power measurement functions of break point

$$(\mathbf{P}_l + j\mathbf{Q}_l)^m = \mathbf{P}_{kl}^x + j\mathbf{Q}_{kl}^x + \mathbf{P}_{nl}^x + j\mathbf{Q}_{nl}^x - \mathbf{A}_{kl}^x \mathbf{Z}_{kl} - \mathbf{A}_{nl}^x \mathbf{Z}_{nl} + j\mathbf{V}_l^2 \mathbf{X}_{cl} \quad (14)$$

Compared with the radial network state estimation model, the meshed network state estimation model has three extra voltage equality constraints on every breakpoint.

3. Observability analysis

For a radial network with n branches, there are $9 * n$ state variables in this estimation model which has more $3 * n$ variables than the conventional estimation method. Actually these extra unknown variables do not need extra measurements to guarantee system observable.

In the radial network, extra $3 * (n - 1)$ voltage constraint measurement functions (defined in Eq. (9)) are included. Thus, $6 * n + 3$ measurement functions are at least needed to solve the proposed estimation model. If all the load pseudo-measurements (including the zero injection) are generated, $6 * n$ measurement functions are provided. If the roots of feeders have voltage measurements, three voltage measurement functions are provided. Then the observability requirement is satisfied. The real-time branch current measurements, other power and voltage measurements can be used to improve the accuracy of estimation results in this method.

For a meshed network with n branches, m loops and $n - m + 1$ nodes, $9 * n$ state variables are used in this estimation method. Besides $3 * n$ voltage constraint measurement functions and $6 * (n - m)$ load pseudo-measurements (including the zero injection) and three voltage measurements on root bus, $6 * m - 3$ extra measurements are needed in this situation. For each loop, two extra branch current (or power) measurements are needed. Fortunately, there are always many real-time current measurements on branches of a loop to monitor whether there is any overload phenomenon in reality. Therefore, this observability requirement can be easily satisfied in meshed distribution system in field application. And other real-time measurements can be used to improve the accuracy of estimation results. This state estimation model can also be used in identifying best location to place meters [15,16].

4. Solution

To solve the estimation model (2), a Lagrange function can be built as:

$$L = J(\mathbf{x}) + \lambda^T \mathbf{c}(\mathbf{x}) \quad (15)$$

The first-order optimality conditions for Lagrange function (15) are derived:

$$\begin{cases} \frac{\partial L}{\partial \mathbf{x}} = \sum_{i=1}^m \frac{\partial \omega_i}{\partial \mathbf{x}} + \sum_{j=1}^p \frac{\partial c_j(\mathbf{x})}{\partial \mathbf{x}} \lambda_j = \mathbf{H}^T \mathbf{W}(\mathbf{x})(\mathbf{z} - \mathbf{h}(\mathbf{x})) + \mathbf{c}^T \lambda = \mathbf{0} \\ \frac{\partial L}{\partial \lambda} = -\mathbf{c}(\mathbf{x}) = \mathbf{0} \end{cases} \quad (16)$$

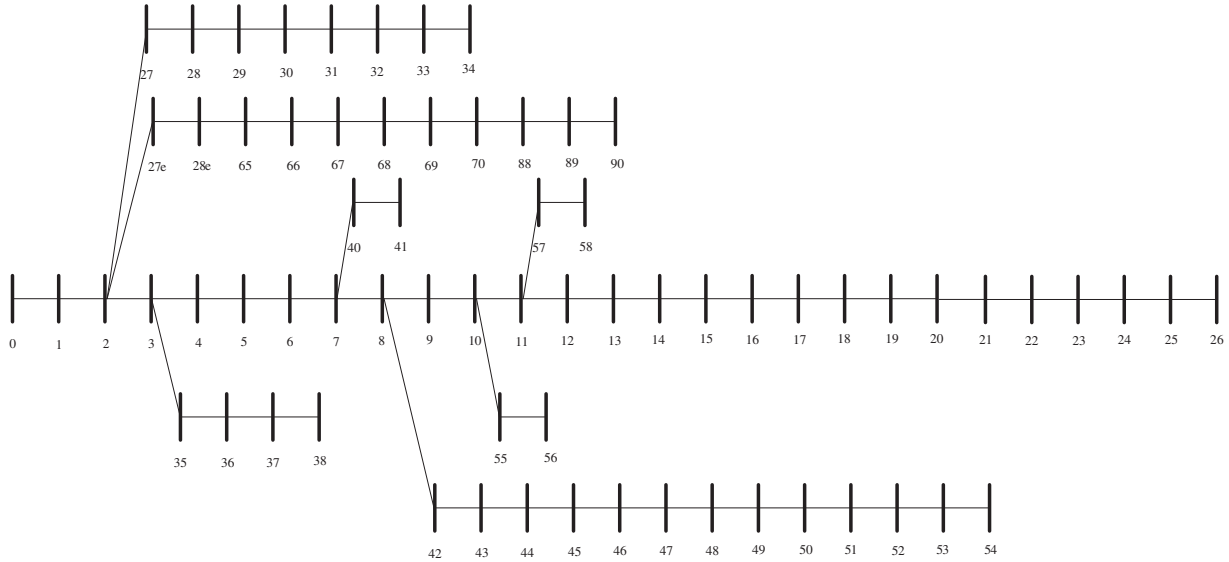


Fig. 5. A 69 nodes radial distribution network.

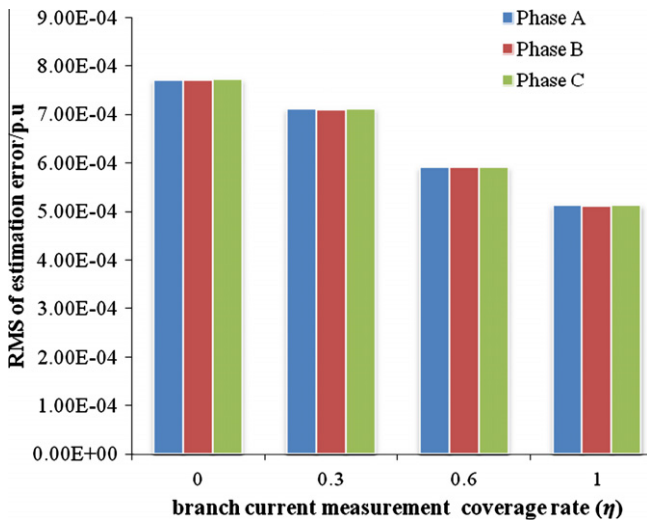


Fig. 6. The RMS of estimation error for load power for Case 1.

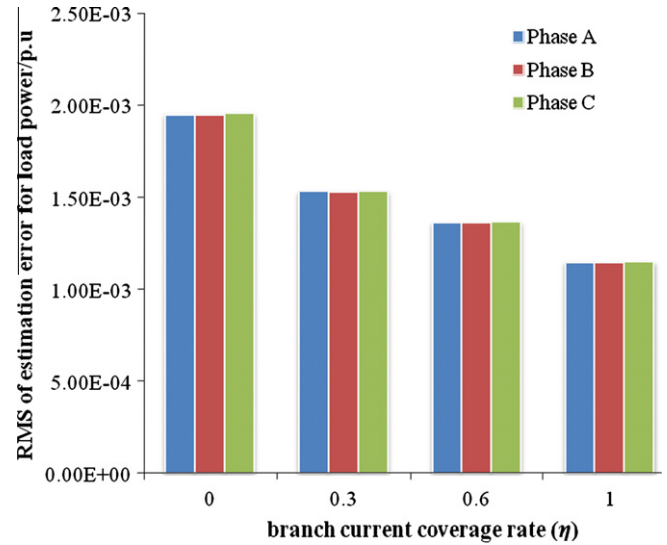


Fig. 7. The RMS of estimation error for load power for Case 2.

where \mathbf{H} is the $m \times n$ measurement Jacobi matrix as used in traditional Weight Least Square state estimation. $\mathbf{W}(\mathbf{x})$ is a $m \times m$ diagonal matrix with the i th diagonal element:

$$W_{ii}(\mathbf{x}) = \omega_i(\mathbf{x})/\sigma^2 \quad (17)$$

and

$$\omega_i(\mathbf{x}) = w_i \exp\left(-\frac{(z_i - h_i(\mathbf{x}))^2}{2\sigma^2}\right) \quad (18)$$

Non-linear algebra Eq. (16) can be solved by Newton method with following differential matrices (Like in the WLS estimator, $\partial\mathbf{H}/\partial\mathbf{x}$ is ignored and an approximate Hessian matrix is used):

$$\frac{\partial^2 L}{\partial \mathbf{x}^2} = -\mathbf{H}^T \mathbf{W} \left[\mathbf{I} - \text{diag}\left\{\frac{(z - \mathbf{h}(\mathbf{x}))^2}{\sigma^2}\right\}\right] \mathbf{H} \quad (19)$$

$$\frac{\partial^2 L}{\partial \lambda \partial \mathbf{x}} = \mathbf{C}$$

\mathbf{C} is the $p \times n$ Jacobi matrix for the zero-injection equation.

The iteration formulation is then as follows:

$$\begin{bmatrix} \mathbf{H}^T \mathbf{W} (\mathbf{I} - \text{diag}\{\frac{(z - \mathbf{h}(\mathbf{x}^{(k)}))^2}{\sigma^2}\}) \mathbf{H} & \mathbf{C}^T \\ \mathbf{C} & \mathbf{0} \end{bmatrix} \begin{bmatrix} \Delta \mathbf{x} \\ -\lambda \end{bmatrix} = \begin{bmatrix} \mathbf{H}^T \mathbf{W} (z - \mathbf{h}(\mathbf{x}^{(k)})) \\ -\mathbf{c}(\mathbf{x}^{(k)}) \end{bmatrix} \quad (20)$$

$$\mathbf{x}^{(k+1)} = \mathbf{x}^{(k)} + \Delta \mathbf{x} \quad (21)$$

Remark 1. Due to the special state variables, all the measurement functions are simple and straightforward. The proposed method has no trigonometric calculation and has a good performance. The interior point optimization method can also be used to solve this estimation model [14].

The condition number of the coefficient matrix in Eq. (20) can be improved by simply scaling the Lagrangian multipliers in (15) [20]:

$$L = \alpha J(\mathbf{x}) + \lambda^T \mathbf{c}(\mathbf{x}) \quad (22)$$

Table 1
Comparison of two different state estimation methods' results for Case 2 at coverage rate $\eta = 1$.

| State estimation method | RMS of load estimation error (Phase A)/p.u | Iteration numbers | Convergence judgment |
|---|--|-------------------|------------------------------------|
| State estimation method with measurement transformation [1] | 1.22E-03 | 5 | $\ \Delta\mathbf{x}\ _2 < 10^{-5}$ |
| State estimation method proposed in this paper | 1.15E-03 | 5 | $\ \Delta\mathbf{x}\ _2 < 10^{-5}$ |

The iteration formulation is then as follows:

$$\begin{bmatrix} \alpha\mathbf{H}^T\mathbf{W}(\mathbf{I} - \text{diag}\{\frac{(z-\mathbf{h}(\mathbf{x}^{(k)}))^2}{\sigma^2}\})\mathbf{H} & \mathbf{C}^T \\ \mathbf{C} & 0 \end{bmatrix} \begin{bmatrix} \Delta\mathbf{x} \\ -\lambda \end{bmatrix} = \begin{bmatrix} \alpha\mathbf{H}^T\mathbf{W}(\mathbf{z} - \mathbf{h}(\mathbf{x}^{(k)})) \\ -\mathbf{c}(\mathbf{x}^{(k)}) \end{bmatrix} \quad (23)$$

where α is chosen as $\alpha = \frac{1}{\max W_{ii}(\mathbf{x})}$.

5. Numerical tests

5.1. Sixty nine nodes distribution system

To illustrate the performance of the proposed method, numerical tests on 69 nodes distribution system with radial and meshed networks were done.

Branch current measurement coverage rate η is defined as:

$$\eta = \frac{n_{m\text{-}branch}}{n_{branch}} \times 100\% \quad (24)$$

where $n_{m\text{-}branch}$ is the number of branch current magnitude measurements, n_{branch} is the total number of branches. Obviously, $\eta = 1$ means each branch has a current measurement.

To characterize the estimation accuracy, the RMS (root of mean square) of estimation error for load power is defined as:

$$r_{Load(\phi)} = \sqrt{\frac{\sum |P_{loadi(\phi)} - P_{loadi(\phi)}^{se}|^2 + \sum |Q_{loadi(\phi)} - Q_{loadi(\phi)}^{se}|^2}{2n_{Load}}} \quad (25)$$

where n_{Load} is the number of loads, $P_{loadi(\phi)}$, $Q_{loadi(\phi)}$ are respectively the true value of the i th load ϕ phase active power and reactive power measurement, $P_{loadi(\phi)}^{se}$, $Q_{loadi(\phi)}^{se}$ are respectively the estimated value of the i th load ϕ phase active power and reactive power measurement.

In the numerical tests, all the measurement errors were randomly generated complying with Gaussian distribution.

$$(z)^m = h_{flow} \cdot (1 + err) \quad (26)$$

where err is random error complying with Gaussian distribution, h_{flow} is the true value from power flow result and $(z)^m$ is measurement value.

Besides current measurements and load pseudo-measurements, the voltage measurement and power measurements are only placed on root nodes and root branches of feeders in the test systems which is consistent with real measurements configuration in reality.

Table 2
Bad measurement data.

| Branch | Type | Measurement value of branch current (Phase A) (A) | Base power flow value (Phase A) (A) | Measurement value (Phase B) (A) | Base power flow value (Phase B) (A) | Measurement value (Phase C) (A) | Base power flow value (Phase C) (A) |
|----------|--------|---|-------------------------------------|---------------------------------|-------------------------------------|---------------------------------|-------------------------------------|
| Ln 36–37 | Ampere | 130.09 | 43.36 | 43.33 | 43.33 | 43.40 | 43.40 |

Table 3
State estimation result (Phase A) with bad data.

| Bus no. | Load true value (Phase A) | | Load estimation result (Phase A) | | Load estimation error (Phase A) | |
|----------|----------------------------------|----------|----------------------------------|----------|--|----------|
| | P (kW) | Q (kVAr) | P (kW) | Q (kVAr) | P (kW) | Q (kVAr) |
| 36 | 64.3 | 56.8 | 64.60 | 58.6 | 0.30 | 1.8 |
| 37 | 128 | 91.5 | 127.00 | 91.8 | -1.00 | 0.3 |
| Branch | Current true value (Phase A) (A) | | Estimation result (Phase A) (A) | | Current estimation error (Phase A) (A) | |
| Ln 36–37 | 43.36 | | 43.37 | | 0.01 | |

The weight of load pseudo-measurements is 0.1, and weight of other measurements are all 100 in the following numerical tests. The convergence criterion of state estimation is defined as $\|\Delta\mathbf{x}\|_2 < 10^{-5}$ and the parameter σ in estimation model is specified as $\sqrt{0.1}$.

5.1.1. Radial network

The 69 nodes distribution system with radial network is shown in Fig. 5 which is firstly presented in Ref. [12]. Based on the original network configuration, capacitors are added on node 18, 47, 52, 58 and 89 respectively and their reactance are all 1068.504 Ω for each phase. The power base $S_B = 10$ MVA and line voltage base $V_B = 12.66$ kV.

Totally three different cases with different measurements errors are generated in this test. In each case there are four tests, with different branch current measurements coverage rates, are calculated to illustrate how branch current measurements improve the estimation results.

Case 1: The error mean value of node voltage, root injection power and branch current measurements is 0 and their error variances is $1e-7$; The error mean value of load pseudo-measurements is 0 and their variance is 0.05. The three phase base power flow results are shown Appendix A Table A1, which are three phase unbalanced. The branch current measurements coverage rates are 0, 0.3, 0.6 and 1 respectively for each test. And the placements of branch current measurements are listed in Appendix A Table A2. The state estimation results at coverage rate $\eta = 1$ are listed in Appendix A Table A3, in which the maximum load state estimation error is 3 kW at bus 50. It can be seen that the estimation results can be very accurate for high branch current measurements coverage rate.

Case 2: The error variance of load pseudo-measurements increases to 0.1, the configuration of other measurements remains unchanged for all the four tests. The RMS of estimation errors of load power ($r_{Load(\phi)}$) for case 1 and case 2 with different branch current measurement coverage rates are shown in Figs. 6 and 7.

It can be seen from Figs. 6 and 7 that the branch current measurements can significantly improve the accuracy of estimation result of load power. The accuracy of load power pseudo-measurements' estimation results increases when the number of branch current measurements grow. Comparing with Figs. 6 and 7, it can be concluded that real-time branch current measurements have better effect on improving the accuracy of load power pseudo-measurements' estimation result for those with larger error variances.

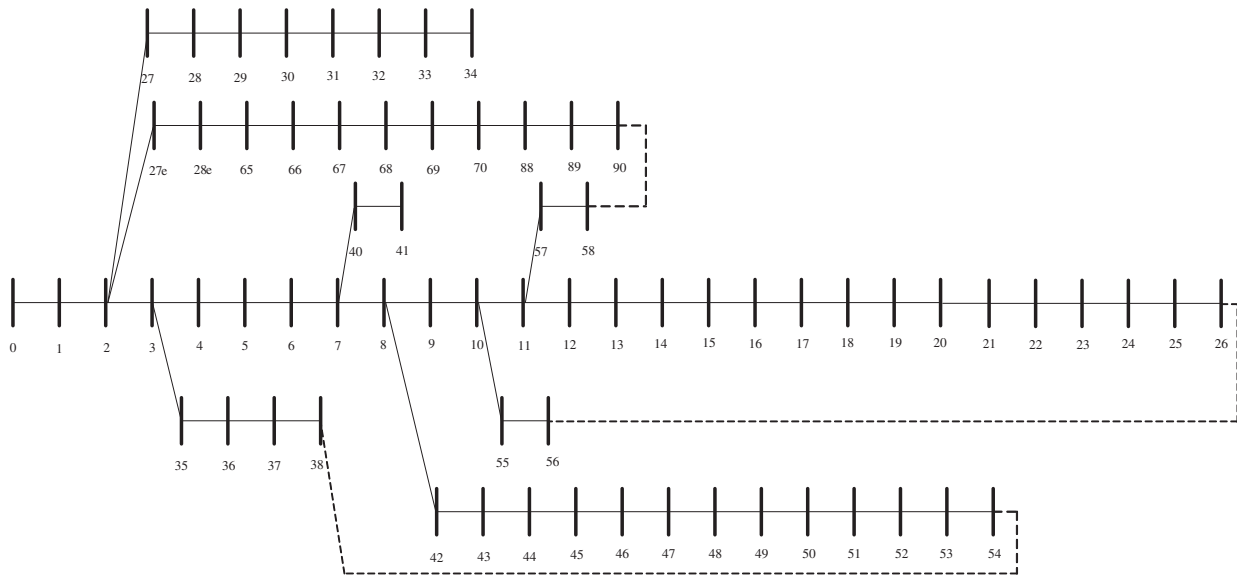


Fig. 8. Sixty nine nodes weak meshed distribution network.

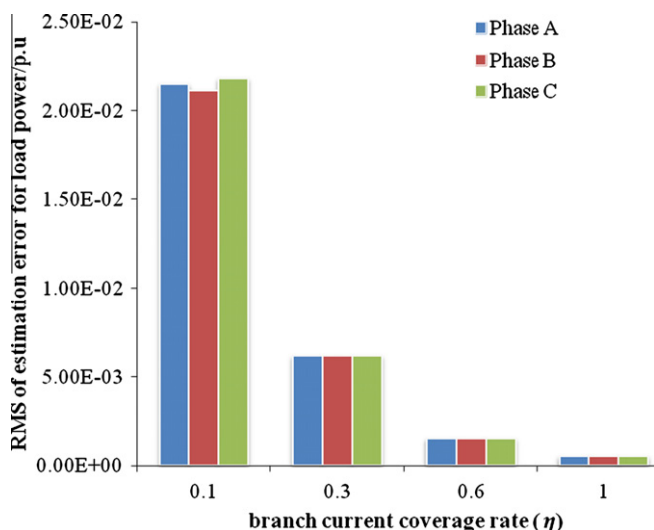


Fig. 9. The RMS of estimation error for meshed distribution network with different branch current measurements coverage rates.

In the state estimation method proposed in [1], all branch current magnitude measurements should be transformed into virtual complex branch current measurements and all load power measurements should be transformed to virtual complex node injection measurements, which may lead to extra estimation error. For the proposed method in this paper, no measurements transformation are needed. These two methods have been tested for Case 2 at coverage rate $\eta = 1$. The results of the two methods are listed in Table 1. From Table 1, it can be seen that the method proposed in this paper can get more accurate results.

Case 3: The measurements configuration is the same as case 1 at coverage rate $\eta = 1$ except that the branch current measurements on the sending end of branch 36–37 are set as bad data. The values of bad data are listed in Table 2.

The state estimation results of the branch current measurements and its interrelated measurements for case 3 are listed in Table 3.

According to the result listed in Table 3, we can see that the proposed estimation method can automatically reject the bad data if the branch current measurements are redundant. Therefore, no

Table 4

Field data of one distribution network in China.

| | Number | Measurement configuration |
|----------|--------|---|
| Nodes | 25,996 | – |
| Feeders | 239 | 239 Voltage magnitude measurements, active and reactive power at the root of feeder |
| Loads | 12,787 | 11,350 Power measurements for each load from AMR |
| Branches | 35,499 | 2141 Branch current magnitude measurements |

Table 5

State estimation results in field application.

| RMS of estimation error for load measurements | | Maximum load measurements estimation error | | RMS of estimation error for branch current measurements (A) | Maximum estimation error for branch current measurements (A) |
|---|----------|--|----------|---|--|
| P (kW) | Q (kVAr) | P (kW) | Q (kVAr) | | |
| 3.14 | 5.51 | 11.5 | 15.5 | 0.09 | 0.23 |

extra bad data identification and rejection module is needed in this method.

5.1.2. Meshed network

A meshed network (shown in Fig. 8) is formed by adding loop branch 38–54, 58–90 and 26–56 of the 69 nodes radial distribution system as shown in Fig. 5. The added loop branches' parameters are shown in Appendix A Table A4.

Four numerical tests with different branch current measurements coverage rates are calculated to demonstrate the performance of the proposed method for meshed network.

In all these tests, the mean values of node voltage, branch current and the root injection power measurements' errors are 0 and their error variances are $1e-7$; Error mean value of load pseudo-measurements is 0 and error variances are 0.01. The placements of branch measurement for different coverage rates are shown in Appendix A Table A5.

The estimation results for tests with different ampere measurement coverages are shown in Fig. 9. It shows the increasing of

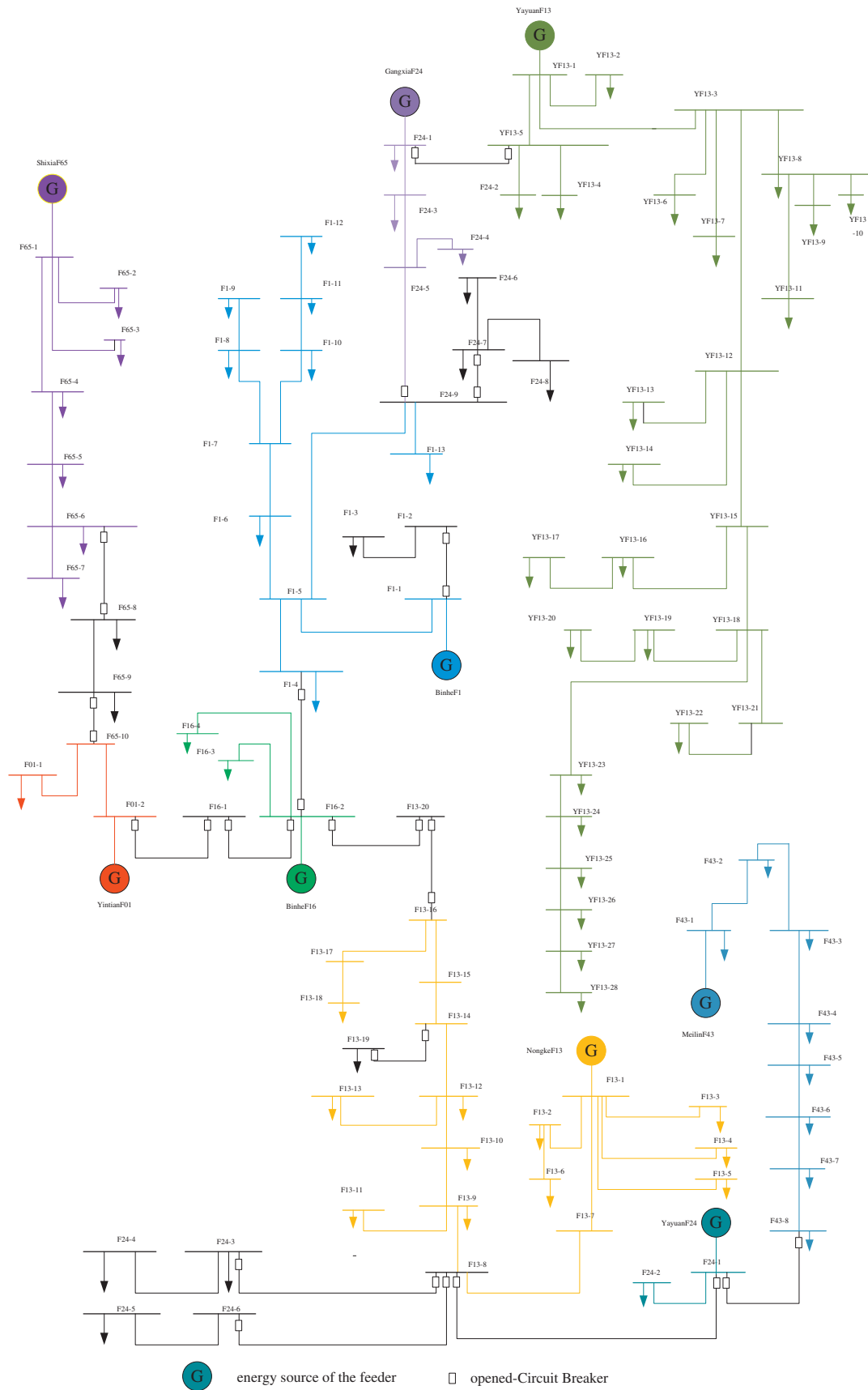


Fig. A1. Part of a real distribution network in China.

branch current measurement coverage rate (η) can significantly improve the accuracy of estimated load power. For weak meshed

network, this method need two extra branch current measurements for each loop. So if the coverage rate $\eta = 0$, which means

no branch current measurements exist, the network will be unobservable in this method. The minimum coverage rate is 0.1 among these tests, in which there are only six branch current measurements and a reasonable estimation results are gotten. From Table A5 in Appendix A, we can see that there exactly two branch current measurements on each loop which can guarantee the network observable. If there are no enough branch current or power measurements, power flow method could be used for load allocation instead of state estimation [8].

5.2. Actual distribution network

To verify the performance of estimator in practical distribution system operation, part of the distribution system for Shenzhen city is used in the test. The test distribution network diagram is figured out in Appendix A Fig. A1 and operates radially. The parameters configuration of distribution network is listed in Table 4. The branch current measurements are real-time measurements collected by SCADA system. Very few PTs have been installed on

Table A1
Base power flow of 69 nodes radial distribution system.

| Bus no. | Phase A | | Phase B | | Phase C | |
|---------|---------|----------|---------|----------|---------|----------|
| | P (kW) | Q (kVAr) | P (kW) | Q (kVAr) | P (kW) | Q (kVAr) |
| 5 | 36.20 | 34.90 | 36.10 | 34.80 | 36.30 | 35.00 |
| 6 | 51.50 | 48.00 | 51.40 | 47.90 | 51.60 | 48.10 |
| 7 | 25.00 | 18.00 | 24.90 | 17.90 | 25.10 | 18.10 |
| 8 | 48.00 | 45.30 | 47.90 | 45.20 | 48.10 | 45.40 |
| 9 | 36.90 | 33.90 | 36.80 | 33.80 | 37.00 | 34.00 |
| 10 | 48.30 | 34.70 | 48.20 | 34.60 | 48.40 | 34.80 |
| 11 | 48.30 | 34.70 | 48.20 | 34.60 | 48.40 | 34.80 |
| 12 | 9.33 | 5.17 | 9.23 | 5.07 | 9.43 | 5.27 |
| 13 | 9.33 | 5.17 | 9.23 | 5.07 | 9.43 | 5.27 |
| 15 | 15.20 | 10.00 | 15.10 | 9.90 | 15.30 | 10.10 |
| 16 | 58.00 | 49.70 | 57.90 | 49.60 | 58.10 | 49.80 |
| 17 | 20.00 | 11.70 | 19.90 | 11.60 | 20.10 | 11.80 |
| 19 | 37.70 | 36.30 | 37.60 | 36.20 | 37.80 | 36.40 |
| 20 | 38.00 | 27.00 | 37.90 | 26.90 | 38.10 | 27.10 |
| 21 | 46.40 | 45.80 | 46.30 | 45.70 | 46.50 | 45.90 |
| 23 | 47.30 | 44.70 | 47.20 | 44.60 | 47.40 | 44.80 |
| 25 | 32.20 | 30.90 | 32.10 | 30.80 | 32.30 | 31.00 |
| 26 | 32.20 | 30.90 | 32.10 | 30.80 | 32.30 | 31.00 |
| 27 | 8.67 | 6.20 | 8.57 | 6.10 | 8.77 | 6.30 |
| 28 | 36.20 | 33.70 | 36.10 | 33.60 | 36.30 | 33.80 |
| 32 | 4.67 | 3.33 | 4.57 | 3.23 | 4.77 | 3.43 |
| 33 | 44.50 | 42.70 | 44.40 | 42.60 | 44.60 | 42.80 |
| 34 | 32.90 | 32.20 | 32.80 | 32.10 | 33.00 | 32.30 |
| 27e | 46.70 | 44.20 | 46.60 | 44.10 | 46.80 | 44.30 |
| 28e | 8.67 | 6.18 | 8.57 | 6.08 | 8.77 | 6.28 |
| 66 | 35.50 | 33.20 | 35.40 | 33.10 | 35.60 | 33.30 |
| 67 | 35.50 | 33.20 | 35.40 | 33.10 | 35.60 | 33.30 |
| 68 | 7.07 | 3.67 | 6.97 | 3.57 | 7.17 | 3.77 |
| 70 | 43.30 | 42.80 | 43.20 | 42.70 | 43.40 | 42.90 |
| 89 | 13.10 | 8.77 | 13.00 | 8.67 | 13.20 | 8.87 |
| 90 | 51.10 | 46.80 | 51.00 | 46.70 | 51.20 | 46.90 |
| 36 | 64.30 | 56.80 | 64.20 | 56.70 | 64.40 | 56.90 |
| 37 | 128.00 | 91.50 | 128.00 | 91.40 | 128.00 | 91.60 |
| 38 | 128.00 | 91.50 | 128.00 | 91.40 | 128.00 | 91.60 |
| 40 | 43.50 | 39.40 | 43.40 | 39.30 | 43.60 | 39.50 |
| 41 | 45.50 | 42.20 | 45.40 | 42.10 | 45.60 | 42.30 |
| 42 | 31.50 | 31.20 | 31.40 | 31.10 | 31.60 | 31.30 |
| 43 | 46.80 | 44.30 | 46.70 | 44.20 | 46.90 | 44.40 |
| 44 | 8.00 | 5.73 | 7.90 | 5.63 | 8.10 | 5.83 |
| 48 | 33.30 | 24.00 | 33.20 | 23.90 | 33.40 | 24.10 |
| 50 | 415.00 | 296.00 | 415.00 | 296.00 | 415.00 | 296.00 |
| 51 | 78.70 | 75.70 | 78.60 | 75.60 | 78.80 | 75.80 |
| 53 | 75.70 | 54.00 | 75.60 | 53.90 | 75.80 | 54.10 |
| 54 | 87.70 | 82.00 | 87.60 | 81.90 | 87.80 | 82.10 |
| 55 | 74.00 | 72.30 | 73.90 | 72.20 | 74.10 | 72.40 |
| 56 | 36.00 | 34.30 | 35.90 | 34.20 | 36.10 | 34.40 |
| 57 | 39.30 | 36.70 | 39.20 | 36.60 | 39.40 | 36.80 |
| 58 | 80.30 | 77.70 | 80.20 | 77.60 | 80.40 | 77.80 |

Table A2

The placements of branch current measurements for different coverage rate η in radial 69 nodes network. (\checkmark means the branch current measurement existed – means not).

| Branch | η | | |
|------------|--------------|--------------|--------------|
| | 1 | 0.6 | 0.3 |
| Ln 2–3 | \checkmark | \checkmark | \checkmark |
| Ln 2–27 | \checkmark | \checkmark | \checkmark |
| Ln 2–27e | \checkmark | \checkmark | \checkmark |
| Ln 3–4 | \checkmark | \checkmark | \checkmark |
| Ln 3–35 | \checkmark | \checkmark | \checkmark |
| Ln 27–28 | \checkmark | \checkmark | \checkmark |
| Ln 27e–28e | \checkmark | \checkmark | \checkmark |
| Ln 5–6 | \checkmark | \checkmark | \checkmark |
| Ln 36–37 | \checkmark | \checkmark | \checkmark |
| Ln 28–29 | \checkmark | \checkmark | \checkmark |
| Ln 28e–65 | \checkmark | \checkmark | \checkmark |
| Ln 6–7 | \checkmark | \checkmark | \checkmark |
| Ln 37–38 | \checkmark | \checkmark | \checkmark |
| Ln 32–33 | \checkmark | \checkmark | \checkmark |
| Ln 66–67 | \checkmark | \checkmark | \checkmark |
| Ln 7–8 | \checkmark | \checkmark | – |
| Ln 7–40 | \checkmark | \checkmark | – |
| Ln 33–34 | \checkmark | \checkmark | – |
| Ln 67–68 | \checkmark | \checkmark | – |
| Ln 8–9 | \checkmark | \checkmark | – |
| Ln 8–42 | \checkmark | \checkmark | – |
| Ln 40–41 | \checkmark | \checkmark | – |
| Ln 68–69 | \checkmark | \checkmark | – |
| Ln 9–10 | \checkmark | \checkmark | – |
| Ln 42–43 | \checkmark | \checkmark | – |
| Ln 70–88 | \checkmark | \checkmark | – |
| Ln 10–11 | \checkmark | \checkmark | – |
| Ln 10–55 | \checkmark | \checkmark | – |
| Ln 43–44 | \checkmark | \checkmark | – |
| Ln 89–90 | \checkmark | \checkmark | – |
| Ln 11–12 | \checkmark | \checkmark | – |
| Ln 11–57 | \checkmark | – | – |
| Ln 55–56 | \checkmark | – | – |
| Ln 44–45 | \checkmark | – | – |
| Ln 12–13 | \checkmark | – | – |
| Ln 57–58 | \checkmark | – | – |
| Ln 47–48 | \checkmark | – | – |
| Ln 13–14 | \checkmark | – | – |
| Ln 48–49 | \checkmark | – | – |
| Ln 15–16 | \checkmark | – | – |
| Ln 50–51 | \checkmark | – | – |
| Ln 16–17 | \checkmark | – | – |
| Ln 51–52 | \checkmark | – | – |
| Ln 17–18 | \checkmark | – | – |
| Ln 52–53 | \checkmark | – | – |
| Ln 18–19 | \checkmark | – | – |
| Ln 53–54 | \checkmark | – | – |
| Ln 19–20 | \checkmark | – | – |
| Ln 20–21 | \checkmark | – | – |
| Ln 21–22 | \checkmark | – | – |
| Ln 23–24 | \checkmark | – | – |
| Ln 25–26 | \checkmark | – | – |

breakers because of limited space, so the number of branch power measurements are very small. The quasi-real-time power measurements of load are generated from the Auto Meter Reading System (AMR), which are updated every 15 min. The accuracy of load power measurements are much lower than the branch current measurements.

The state estimation results are listed in Table 5. It can be seen from Table 5 that the estimation results are fairly accurate for monitoring and decision making.

6. Conclusion

In this paper, a novel state estimation method is proposed for distribution system with large number of current measurements. This method has following characteristics:

Table A3
Load estimation results for radial distribution at coverage rate $\eta = 1$.

| Bus no. | True value (Phase A) (1) | | Meas. | | Estimated result (Phase A) (2) | | Meas. est. error (2)–(1) | |
|---------|--------------------------|----------|--------|----------|--------------------------------|----------|--------------------------|----------|
| | P (kW) | Q (kVAr) | P (kW) | Q (kVAr) | P (kW) | Q (kVAr) | P (kW) | Q (kVAr) |
| 5 | 36.2 | 34.9 | 37.40 | 36.10 | 36 | 34.9 | -0.2 | 0 |
| 6 | 51.5 | 48 | 53.40 | 49.80 | 51.3 | 48.1 | -0.2 | 0.1 |
| 7 | 25 | 18 | 25.60 | 18.40 | 23.7 | 16.9 | -1.3 | -1.1 |
| 8 | 48 | 45.3 | 50.90 | 48.10 | 48.2 | 46 | 0.2 | 0.7 |
| 9 | 36.9 | 33.9 | 37.00 | 33.90 | 36 | 33.2 | -0.9 | -0.7 |
| 10 | 48.3 | 34.7 | 51.10 | 36.60 | 48.6 | 34.8 | 0.3 | 0.1 |
| 11 | 48.3 | 34.7 | 49.20 | 35.30 | 47.2 | 33.7 | -1.1 | -1 |
| 12 | 9.33 | 5.17 | 9.63 | 5.33 | 8.6 | 4.49 | -0.73 | -0.68 |
| 13 | 9.33 | 5.17 | 9.48 | 5.25 | 8.65 | 4.56 | -0.68 | -0.61 |
| 15 | 15.2 | 10 | 16.20 | 10.70 | 14.9 | 9.62 | -0.3 | -0.38 |
| 16 | 58 | 49.7 | 61.20 | 52.40 | 59.2 | 50.8 | 1.2 | 1.1 |
| 17 | 20 | 11.7 | 20.90 | 12.20 | 19.4 | 11 | -0.6 | -0.7 |
| 19 | 37.7 | 36.3 | 39.40 | 38.00 | 37.9 | 36.8 | 0.2 | 0.5 |
| 20 | 38 | 27 | 38.00 | 27.00 | 36.7 | 26 | -1.3 | -1 |
| 21 | 46.4 | 45.8 | 48.50 | 47.90 | 47 | 46.7 | 0.6 | 0.9 |
| 23 | 47.3 | 44.7 | 49.40 | 46.60 | 47.9 | 45.4 | 0.6 | 0.7 |
| 25 | 32.2 | 30.9 | 32.90 | 31.60 | 31.5 | 30.4 | -0.7 | -0.5 |
| 26 | 32.2 | 30.9 | 32.90 | 31.60 | 31.5 | 30.4 | -0.7 | -0.5 |
| 27 | 8.67 | 6.2 | 8.68 | 6.21 | 7.97 | 5.57 | -0.7 | -0.63 |
| 28 | 36.2 | 33.7 | 36.40 | 33.90 | 35.6 | 33.2 | -0.6 | -0.5 |
| 32 | 4.67 | 3.33 | 4.76 | 3.40 | 3.96 | 2.68 | -0.71 | -0.65 |
| 33 | 44.5 | 42.7 | 45.40 | 43.50 | 44.5 | 42.7 | 0 | 0 |
| 34 | 32.9 | 32.2 | 34.80 | 34.10 | 33.9 | 33.3 | 1 | 1.1 |
| 27e | 46.7 | 44.2 | 47.80 | 45.20 | 46.9 | 44.5 | 0.2 | 0.3 |
| 28e | 8.67 | 6.18 | 8.89 | 6.34 | 8.09 | 5.63 | -0.58 | -0.55 |
| 66 | 35.5 | 33.2 | 37.10 | 34.70 | 36.2 | 33.9 | 0.7 | 0.7 |
| 67 | 35.5 | 33.2 | 36.50 | 34.10 | 35.7 | 33.4 | 0.2 | 0.2 |
| 68 | 7.07 | 3.67 | 7.19 | 3.73 | 6.45 | 3.04 | -0.62 | -0.63 |
| 70 | 43.3 | 42.8 | 43.30 | 42.80 | 42.6 | 42.1 | -0.7 | -0.7 |
| 89 | 13.1 | 8.77 | 13.70 | 9.21 | 13 | 8.52 | -0.1 | -0.25 |
| 90 | 51.1 | 46.8 | 52.10 | 47.70 | 51.3 | 47 | 0.2 | 0.2 |
| 36 | 64.3 | 56.8 | 66.30 | 58.60 | 64.5 | 57.1 | 0.2 | 0.3 |
| 37 | 128 | 91.5 | 129.00 | 91.80 | 127 | 90.4 | -1 | -1.1 |
| 38 | 128 | 91.5 | 131.00 | 93.60 | 129 | 92.1 | 1 | 0.6 |
| 40 | 43.5 | 39.4 | 45.70 | 41.50 | 43.8 | 39.9 | 0.3 | 0.5 |
| 41 | 45.5 | 42.2 | 48.00 | 44.50 | 46 | 42.9 | 0.5 | 0.7 |
| 42 | 31.5 | 31.2 | 33.40 | 33.10 | 30.5 | 30.9 | -1 | -0.3 |
| 43 | 46.8 | 44.3 | 54.60 | 51.70 | 48 | 47.2 | 1.2 | 2.9 |
| 44 | 8 | 5.73 | 8.48 | 6.07 | 7.78 | 5.19 | -0.22 | -0.54 |
| 48 | 33.3 | 24 | 33.80 | 24.30 | 33.5 | 23.5 | 0.2 | -0.5 |
| 50 | 415 | 296 | 422.00 | 301.00 | 418 | 298 | 3 | 2 |
| 51 | 78.7 | 75.7 | 79.50 | 76.50 | 76.4 | 73.7 | -2.3 | -2 |
| 53 | 75.7 | 54 | 80.50 | 57.40 | 77.2 | 54.5 | 1.5 | 0.5 |
| 54 | 87.7 | 82 | 89.70 | 83.90 | 86.5 | 81.1 | -1.2 | -0.9 |
| 55 | 74 | 72.3 | 77.80 | 76.00 | 75.3 | 74.1 | 1.3 | 1.8 |
| 56 | 36 | 34.3 | 36.70 | 35.00 | 34.2 | 33.1 | -1.8 | -1.2 |
| 57 | 39.3 | 36.7 | 42.50 | 39.60 | 40.2 | 37.9 | 0.9 | 1.2 |
| 58 | 80.3 | 77.7 | 82.70 | 80.00 | 80.5 | 78.3 | 0.2 | 0.6 |

- (1) The branch current measurements, voltage and power measurements are all directly formulated in this method without measurements transformation. Therefore, it is suitable to be used in distribution system with large number of branch current measurements.
- (2) The power on sending end of branch and the square of branch current magnitude are chosen as the state variables, which make the measurement functions simple and easy to be solved.

Table A5
The placements of branch current measurements for different coverage rate η in weak meshed 69 nodes network (\checkmark means the branch current measurement existed – means not).

| Branch name | η | | | |
|-------------|--------------|--------------|--------------|--------------|
| | 1 | 0.6 | 0.3 | 0.1 |
| Ln 2–3 | \checkmark | \checkmark | \checkmark | - |
| Ln 2–27 | \checkmark | \checkmark | \checkmark | - |
| Ln 2–27e | \checkmark | \checkmark | \checkmark | - |
| Ln 3–4 | \checkmark | \checkmark | \checkmark | - |
| Ln 3–35 | \checkmark | \checkmark | \checkmark | - |
| Ln 27–28 | \checkmark | \checkmark | \checkmark | - |
| Ln 27e–28e | \checkmark | \checkmark | \checkmark | - |
| Ln 5–6 | \checkmark | \checkmark | \checkmark | - |
| Ln 36–37 | \checkmark | \checkmark | \checkmark | - |
| Ln 28–29 | \checkmark | \checkmark | \checkmark | - |
| Ln 28e–65 | \checkmark | \checkmark | \checkmark | - |
| Ln 6–7 | \checkmark | \checkmark | \checkmark | - |
| Ln 37–38 | \checkmark | \checkmark | \checkmark | - |
| Ln 32–33 | \checkmark | \checkmark | \checkmark | - |
| Ln 66–67 | \checkmark | \checkmark | \checkmark | - |
| Ln 7–8 | \checkmark | \checkmark | \checkmark | - |
| Ln 7–40 | \checkmark | \checkmark | - | - |
| Ln 38–54 | \checkmark | \checkmark | - | - |
| Ln 33–34 | \checkmark | \checkmark | - | - |
| Ln 67–68 | \checkmark | \checkmark | - | - |
| Ln 8–9 | \checkmark | \checkmark | - | - |
| Ln 8–42 | \checkmark | \checkmark | - | - |
| Ln 40–41 | \checkmark | \checkmark | - | - |
| Ln 53–54 | \checkmark | \checkmark | - | - |
| Ln 68–69 | \checkmark | \checkmark | - | - |
| Ln 9–10 | \checkmark | \checkmark | - | - |
| Ln 42–43 | \checkmark | \checkmark | - | - |
| Ln 52–53 | \checkmark | \checkmark | - | - |
| Ln 70–88 | \checkmark | \checkmark | - | - |
| Ln 10–11 | \checkmark | \checkmark | - | - |
| Ln 10–55 | \checkmark | \checkmark | - | - |
| Ln 43–44 | \checkmark | - | - | - |
| Ln 51–52 | \checkmark | - | - | - |
| Ln 89–90 | \checkmark | \checkmark | \checkmark | \checkmark |
| Ln 11–12 | \checkmark | - | - | - |
| Ln 11–57 | \checkmark | - | - | - |
| Ln 55–56 | \checkmark | - | - | - |
| Ln 44–45 | \checkmark | - | - | - |
| Ln 50–51 | \checkmark | - | - | - |
| Ln 12–13 | \checkmark | - | - | - |
| Ln 57–58 | \checkmark | - | - | - |
| Ln 26–56 | \checkmark | - | - | - |
| Ln 47–48 | \checkmark | \checkmark | \checkmark | \checkmark |
| Ln 49–50 | \checkmark | \checkmark | \checkmark | \checkmark |
| Ln 13–14 | \checkmark | \checkmark | - | - |
| Ln 58–90 | \checkmark | \checkmark | \checkmark | \checkmark |
| Ln 25–26 | \checkmark | - | - | - |
| Ln 15–16 | \checkmark | - | - | - |
| Ln 24–25 | \checkmark | - | - | - |
| Ln 16–17 | \checkmark | - | - | - |
| Ln 22–23 | \checkmark | - | - | - |
| Ln 17–18 | \checkmark | - | - | - |
| Ln 20–21 | \checkmark | \checkmark | \checkmark | \checkmark |
| Ln 18–19 | \checkmark | - | - | - |
| Ln 19–20 | \checkmark | \checkmark | \checkmark | \checkmark |

- (3) This method can be used in radial and meshed distribution systems.

Table A4
Added loop branches' parameters for meshed 69 nodes network.

| Branch name | From bus | To bus | Resistance (Phase A) (Ω) | Reactance (Phase A) (Ω) | Resistance (Phase B) (Ω) | Reactance (Phase B) (Ω) | Resistance (Phase C) (Ω) | Reactance (Phase C) (Ω) |
|-------------|----------|--------|-----------------------------------|----------------------------------|-----------------------------------|----------------------------------|-----------------------------------|----------------------------------|
| Ln 58–90 | 58 | 90 | 0.71 | 0.24 | 0.71 | 0.24 | 0.71 | 0.24 |
| Ln 38–54 | 38 | 54 | 0.71 | 0.24 | 0.71 | 0.24 | 0.71 | 0.24 |
| Ln 26–56 | 26 | 56 | 0.71 | 0.24 | 0.71 | 0.24 | 0.71 | 0.24 |

- (4) This method can automatically reject the bad data when the branch current measurements become redundant, which makes sure of robust state estimation with unbiased bad data [17].

Due to the limitation of space in city, few PTs are installed in MV urban distribution network. Therefore, there are few real-time power and voltage measurements while the branch current measurements are dominant. This method is designed for this situation and has a good performance.

Acknowledgements

This work was supported in part by the National Science Foundation of China (50707013) and Program for New Century Excellent Talents in University (NCET-11-0281).

Appendix A

See Fig. A1 and Tables A1–A5.

References

- [1] Lu CN, Teng JH, Liu W-H. Distribution system state estimation. *IEEE Trans Power Syst* 1995;10(1):229–40.
- [2] Lin Whei-Min, Teng Jen-Hao. State estimation for distribution systems with zero-injection constraints. *IEEE Trans Power Syst* 1996;11(1):518–24.
- [3] Baran Mesut E, Kelly Arther W. A branch-current based state estimation method for distribution systems. *IEEE Trans Power Syst* 1995;10(1):483–91.
- [4] Wang Haibin, Schulz Noel N. A revised branch current-based distribution system state estimation algorithm and meter placement impact. *IEEE Trans Power Syst* 2004;19(1):207–13.
- [5] Sun Hongbin, Zhang Boming, Xiang Niande. A branch-power-based state estimation method for distribution systems. *Autom Electr Power Syst* 1998;22(8):12–6. in Chinese.
- [6] Deng Youman, He Ying, Zhang Boming. A branch-estimation-based state estimation method for radial distribution systems. *IEEE Trans Power Syst* 2002;17(4):1057–62.
- [7] Singh R, Pal BC, Jabr RA. Distribution system state estimation through Gaussian mixture model of the load as pseudo-measurement. *IET Gener Transm Distrib* 2010;4(1):50–9.
- [8] Miranda Vladimiro, Pereira Jorge, Saraiva Joao Tome. Load allocation in DMS with a fuzzy state estimator. *IEEE Trans Power Syst* 2000;15(2):529–34.
- [9] Meldorf M, Treufeldt U, Kilter J. State estimation technique for distribution networks. *Power Tech IEEE Russia* 2005:1–5.
- [10] Ghosh AK, Lubkeman DL, Jones RH. Load modeling for distribution circuit state estimation. *IEEE Trans Power Deliv* 1997;12(2):999–1005.
- [11] Shirmohammadi D, Hong HW, Semlyen A, et al. A compensation-based power flow method for weakly meshed distribution and transmission networks. *IEEE Trans Power Syst* 1988;3(2):753–61.
- [12] Baran Mesut E, Felix F Wu. Network reconfiguration in distribution systems for loss reduction and load balancing. *IEEE Trans Power Deliv* 1989;4(2):1401–7.
- [13] Expósito Antonio Gómez, Villa Jaén Antonio de la, Ramírez Izaga Jorge L. An alternative state estimation formulation for radial distribution. In: *Proceedings of the IEEE power Tech'07, Lausanne; July 2007*. p. 396–400.
- [14] Rakpenthai Chawasak, Premrudeepreechacharn Suttichai, Uatrongjit Sermsak Watson, Neville R. An interior point method for WLAV state estimation of power system with UPFCs. *Int J Electr Power Energy Syst* 2010;32:671–7.
- [15] Ramesh L, Chakraborty N, Chowdhury SP, Chowdhury S. Intelligent DE algorithm for measurement location and PSO for bus voltage estimation in power distribution system. *Int J Electr Power Energy Syst* 2012;39:1–8.
- [16] Razi Kazemi AA, Dehghanian P. A practical approach on optimal RTU placement in power distribution systems incorporating fuzzy sets theory. *Int J Electr Power Energy Syst* 2012;37:31–42.
- [17] Singh D, Misra RK, Singh VK, Pandey RK. Bad data pre-filter for state estimation. *Int J Electr Power Energy Syst* 2010;32:1165–74.
- [20] Abur A, Expósito AG. *Power system state estimation: theory and implementation*. New York: Arcel Dekker; 2004. pp. 50–73.